Discovery of unknown quorum-sensing reprogramming factors in *Pseudomonas aeruginosa* using a dual-acting-gene-blocking approach

Wenjie Cai[1,2], Huiming Liao[1,2], Mingqi Lu[1,2], Xiangting Zhou[1,2], Xiaoyan Cheng[1,2], Weijun Dai[1,2]

[1]Guangdong Laboratory for Lingnan Modern Agriculture, South China Agricultural University, Guangzhou, 510642, China

[2]College of Plant Protection, Integrative Microbiology Research Center, South China Agricultural University, Guangzhou, 510642, China

Send correspondence to: Weijun Dai

Integrative Microbiology Research Center, South China of Agricultural University, Guangzhou, 510642, China

daiweijun@scau.edu.cn

Running title: identification of QS-reprogramming determinants

Key words: quorum sensing, LasR, *Pseudomonas aeruginosa*

ABSTRACT

LasR-null, QS-active mutants commonly appear in *Pseudomonas aeruginosa* isolates from chronically infected cystic fibrosis (CF) lung patients. However, underlying QS-reprogramming factors in CF isolates have yet to be uncovered. Here, we developed an unconventional screening approach, named dual-acting-gene-blocking (DAGB), to identify unknown QS-reprogramming determinants. Mutations in *mexT* have been linked to QS-reprogramming in the laboratory PAO1 LasR-null mutant. To block the inactivation of MexT, we engineered a recombinant LasR-null strain by introducing another copy of wild-type *mexT* into the neutral site of the genome. This strategy presumably ensures at least one copy of *mexT* is functioning if another one is inactive during the QS-required evolution, which thus blocks the inactivating MexT-mediated QS activation. Using DAGB, we identified a point mutation in *rpoA* (T262->A, RpoA*), encoding the α-subunit of RNA polymerase (RNAP), which could rewire QS activity in the LasR-null background. Like the MexT mutant, RpoA* also activated QS by suppressing the expression of the MexEF-OprN efflux pump. In contrast to the MexT mutant, RpoA* caused milder repression of the MexEF-OprN pump, resulting in an intermediate QS-active phenotype and a slower decline rate of growth fitness when treated with chloramphenicol. With iterative applications of the DAGB-based approach, we further discovered other non-*mexT* determinants capable of rewiring QS. Our study first reports non-MexT QS-reprogramming regulators in the LasR-null mutant, shedding light on understanding the QS activation mechanism in those *P. aeruginosa* LasR-null, QS-active clinical isolates. Our findings demonstrate that DAGB is a productive avenue to rapidly identify unknown genetic determinants in *P. aeruginosa*. Most importantly, the established DAGB-based framework is generalizable and could potentially be extended to uncover untapped pathways in other research areas as well as other organisms.

Introduction

Pseudomonas aeruginosa is an opportunistic pathogen that causes severe acute and chronic human infections in cystic fibrosis (CF) patients with compromised immune systems (Gellatly and Hancock, 2013; Klockgether and Tümmler, 2017). A cohort of *P. aeruginosa* virulence factors is under the control of the quorum-sensing (QS) system (Lee and Zhang, 2015; Papenfort and Bassler, 2016). QS is a bacterial cell-cell communication system that regulates the expression levels of hundreds of genes in a cell density-dependent manner (Lee and Zhang, 2015). *P. aeruginosa* has two acyl-homoserine lactone (AHL) QS systems, Las and Rhl QS systems. In the Las QS system, LasI catalyzes the diffusible QS signal *N*-3-oxododecanoyl homoserine lactone (3OC12-HSL), while LasR binds to the 3OC12-HSL forming a protein-signal complex. This active 3OC12-HSL-LasR complex further activates Las-regulon genes. Similarly, Rhl QS contains an RhlI-RhlR pair, with RhlI synthesizing the butyryl-HSL (C4-HSL) and the C4-HSL-bound RhlR activating the Rhl-regulon. These two AHL QS systems further interact with another Pseudomonas Quinolone Signal (PQS) system, forming a QS hierarchy. In general, Las QS is atop the QS hierarchy, and disruption of either LasI or LasR diminishes the expression of QS-activated genes.

P. aeruginosa genome encodes several resistance-nodulation-division (RND) efflux pumps that transport small molecules into the extracellular environment. MexEF-OprN efflux pumps regulate the QS system by exporting the signaling molecule PQS (Köhler et al., 2001). Overexpression of MexEF-OprN was found in the *nfxC*-type mutants, displaying strongly reduced QS-related phenotypes (Ko¨ hler et al., 1997; Köhler et al., 2001). As a LysR-type transcriptional regulator, MexT is encoded upstream of the *mexEF*-

80 *oprN* operon and positively regulates the expression of this operon (Köhler et al., 1999). Overexpression
81 of MexT substantially decreases QS-controlled products, including C4-HSL, hydrogen cyanide, elastase,
82 pyocyanin and rhamnolipids (Köhler et al., 2001; Tian et al., 2009b). MexT itself is negatively regulated
83 by its neighboring gene *mexS* (Richardot et al., 2016; Sobel et al., 2005). In addition to the *mexEF-oprN*
84 operon, MexT also globally regulates more than 40 genes (Tian et al., 2009a; Tian et al., 2009b).
85 Mutations in the *mexT* gene were identified in isolates obtained from chronic CF lungs and other
86 infections (Gilbert et al., 2012; Smith et al., 2006), and they appeared in *P. aeruginosa* laboratory strains
87 (Cheng et al., 2022; Luong et al., 2014).
88
89 LasR mutants are commonly identified in CF chronic infections (Feltner et al., 2016; Hoffman et al.,
90 2009; Smith et al., 2006). Intriguingly, many LasR-null clinical isolates remain QS activity, producing
91 QS molecules and QS-controlled virulence products, such as C4-HSL and pyocyanin (Bjarnsholt et al.,
92 2010; Chen et al., 2019; Cruz et al., 2020; Feltner et al., 2016). Inactivation of MexT was found to
93 reprogram QS activity in the laboratory strain PAO1 LasR-null background (Kostylev et al., 2019; Oshri
94 et al., 2018) by diminishing the expression of the MexEF-OprN efflux pump that regulates QS activity
95 (Köhler et al., 2001; Tian et al., 2009b). Likewise, disruption of the MexEF-OprN pump also produces
96 similar QS-active phenotypes (Kostylev et al., 2019). Since inactivation of MexT produces active Rhl
97 and PQS QS activities (Kostylev et al., 2019; Oshri et al., 2018), deletion of RhlR abolished the QS
98 activity. However, the deletion of PqsA and/or PqsE only partially attenuated the QS activity (Kostylev
99 et al., 2019). Although mutations in *mexT* were shown to be critical for QS-reprogramming in the
100 laboratory strain, they were rare in clinical isolates (Smith et al., 2006). For example, a LasR-null isolate
101 from CF chronic infection showed QS-active phenotypes, while containing a functioning MexT (Cruz et
102 al., 2020). Therefore, in those LasR-null, QS-active clinical isolates, it is not MexT but other unknown
103 factors that control QS-reprogramming.
104
105 To identify genetic determinants in those LasR-null, QS-active isolates, we here developed a dual-acting-
106 gene-blocking (DAGB) approach. We hypothesized that if the inactivation of MexT is not available,
107 alternative pathways of the bacterium could be selected to operate for QS-reprogramming. Based on this
108 hypothesis, we generated a recombinant LasR-null mutant bearing two copies of functioning *mexT*. We
109 assumed that either copy of two *mexT* genes being mutated would still leave another functioning one
110 during the evolution. Using the DAGB approach, our study identified a RpoA mutant (T262->A, RpoA*)
111 capable of activating QS in the LasR-null background. RNA-seq analysis revealed a QS-active
112 transcriptome profile in the LasR-null-RpoA* mutant, showing elevated expression levels in Rhl- and
113 PQS-related genes. Compared to the MexT mutation, RpoA* had a modest decrease in the expression of
114 the MexEF-OprN efflux pump, resulting from a weaker binding of RNAP to the efflux pump promoter.
115 The RpoA*-mediated modulation of the efflux pump led to an intermediate level of QS phenotypes and
116 a slower decline rate of growth fitness in the presence of chloramphenicol. With further iterative
117 applications of the DAGB-based approach, our study additionally identified GshA and MexE as QS-
118 reprogramming factors. Our work first established a powerful framework for uncovering unknown QS-
119 reprogramming factors in *P. aeruginosa*. Moreover, DAGB developed here could potentially be broadly
120 applied to reveal unknown fields in a given stress environment as well as in different organisms.
121
122 **Results**
123 ***mexT* and *lasR* mutations are not statistically associated in *P. aeruginosa* chronical CF isolates**

124 LasR mutants are common in *P. aeruginosa* CF isolates from chronic infection patients, which often
125 contain an active Rhl QS (Bjarnsholt et al., 2010; Feltner et al., 2016). Through an in vitro evolution
126 approach, *mexT* mutations were found to be responsible for the active Rhl QS in the laboratory PAO1
127 LasR-null mutant strain (Kostylev et al., 2019; Oshri et al., 2018). However, it is unclear whether this
128 laboratory-based finding applies to clinical isolates. To address this concern, we re-analyzed previously
129 published whole genome sequencing (WGS) data of chronical CF infection isolates to investigate a
130 possible correlation between *lasR* and *mexT* mutations. Among 29 CF patients examined, *lasR* mutations,
131 including nonsynonymous single nucleotide substitutions and insertions, were identified in isolates from
132 22 (75.9%) patients. However, only two (9.1%) of those isolates simultaneously had nonsynonymous
133 mutations in *lasR* and *mexT* (Fisher's exact test, $P = 0.23$, odds ratio = 0.27). Moreover, *mexT* mutations
134 were additionally found in some isolates that contain an intact *lasR* (Table S1). Recently, Cruz et al.
135 reported a chronical CF infection isolate (strain E90) (Cruz et al., 2020). This LasR-null isolate E90
136 exhibits typical Rhl-active phenotypes, while containing a complete, functioning MexT. Combined with
137 above findings, *mexT* mutations are not statistically colocalized with *lasR* mutations in those chronically
138 infected CF isolates. Therefore, inactivating MexT might not account for the rewired QS activity at least
139 in some LasR-null, Rhl-active clinical isolates.
140
141 **Development of a systematic approach for identifying none-*mexT* QS-reprograming factors**
142 To explore uncharacterized QS factors responsible for QS hierarchy reprogramming in the LasR-null
143 background, we first tried the traditional transposon mutagenesis approach. A *mariner*-based transposon
144 (pBT20) (Kulasekara et al., 2005) was used to construct the insertion mutant library. This library was
145 screened on the skim milk plate for the visualization of the QS-controlled proteolytic activity.
146 Transposon-inserted genes encoding QS negative regulators, such as *mexT*, would be expected to give
147 rise to QS-active phenotypes. A total of 40, 000 mutant colonies, corresponding to a transposon density
148 of about 156 bp per insertion in the PAO1 genome, were examined. By this way, we could only obtain
149 one transposon colony exhibiting a protease-positive phenotype. This colony has a transposon insertion
150 in the *mexF* gene, which codes for an essential component of the MexEF-OprN efflux pump. Given that
151 MexT-mediated QS-reprogramming mostly relies on the MexEF-OprN efflux pump (Kostylev et al.,
152 2019), it is not surprising to see that the disruption of MexF resulted in a QS-active phenotype. No other
153 QS-reprogramming genetic elements were identified using this approach in our study.
154
155 To circumvent the limitations of transposon mutagenesis, we developed a dual-acting-gene-blocking
156 (DAGB) approach (Fig. 1). Briefly, another *mexT* DNA fragment was integrated into the neutral site of
157 the genome, forming the dual-acting-*mexT*. Under QS-required evolution conditions, *P. aeruginosa*
158 rapidly and spontaneously mutates *mexT* to activate QS in the LasR-null mutant (Kostylev et al., 2019;
159 Oshri et al., 2018). Our DAGB strategy could ensure at least one functioning *mexT* if another copy of
160 *mexT* is mutated in the course of stress evolution. Considering *P. aeruginosa* has an intriguing capacity
161 for adapting to environments through frequent genome variations (Huang et al., 2019), we hypothesized
162 that DAGB would encourage the bacterium to switch to alternative regulatory pathways, i.e. none-*mexT*
163 QS-regulators, to achieve rapid QS activation. Through the evolution of the dual-acting-*mexT*-containing
164 LasR-null mutant and the screening of QS-active single colonies, previously unknown none-*mexT*
165 genetic elements could be identified through localization of the spontaneous mutations.
166
167 **Evolution of the recombinant LasR-null mutant and screening of QS-active colonies**

168 The recombinant LasR-null mutant bearing dual-acting *mexT* was routinely evolved in the casein-based
169 broth, in which QS is activated to produce extracellular proteases required for cell growth (Diggle et al.,
170 2007; Sandoz et al., 2007). Evolving cells were isolated and screened for QS-active phenotypes. Clear
171 evolving cells started to turn turbid at 25d, implying the event of genome adaptation that allows for the
172 production of QS-controlled proteases (Fig. 2). QS activation was confirmed by the elevated pyocyanin
173 in separated protease-positive colonies. Sequencing of *mexT* in those colonies also validated that at least
174 one copy of *mexT* is intact. Therefore, it was not the inactivation of MexT, but other unknown factors
175 that triggered the QS activation. Our results also suggest that *mexT* is not the unique determinant for QS-
176 reprogramming.
177
178 **The mutation in *rpoA* leads to QS activation**
179 To identify occurring mutations in those protease-positive colonies, we selected three of them for whole-
180 genome re-sequencing (WGS). The WGS result revealed that they all bear a common single nucleotide
181 mutation (T4754641->C, T262->A) in *rpoA* (Table S2 and S3), which encodes an α-subunit of RNA
182 polymerase (RNAP). We therefore focused on *rpoA* in the following study. Since *rpoA* is functionally
183 essential for cell viability in *P. aeruginosa* (Lee et al., 2015), in-frame deletion of *rpoA* is not available.
184 To elucidate the roles of *rpoA* in QS regulation, we introduced the same point mutation (T262 ->A) into
185 the LasR-null mutant, generating the LasR-RpoA-T262A mutant (hereafter designated as LasR-RpoA*).
186 The incorporation of RpoA* activated QS in the LasR-null background, showing QS-active phenotypes,
187 including elevated productions of pyocyanin, C4-HSL and PQS as well as cell killing activity (Fig. 3,
188 Fig. S2 and Fig. S3). We noted that QS activity detected in the LasR-RpoA* mutant is higher than the
189 LasR-null mutant, while lower than the LasR-MexT mutant. On the other hand, complementation of an
190 episomal copy of wild-type *rpoA* diminished the QS-controlled proteolysis and pyocyanin yield in the
191 LasR-RpoA* mutant (Fig. S1). Through DAGB, our study first reports RpoA as a novel QS-
192 reprogramming regulator.
193
194 **The LasR-RpoA* mutant exhibits a QS-active transcriptome profile**
195 To investigate the regulatory basis of RpoA* in reprogramming QS, we performed an RNA-seq analysis.
196 Overall, global expression changes were induced in the LasR-RpoA* mutant, with a total of 182 genes
197 differentially expressed (at least a 2-fold change, $P < 0.05$) (Fig. 4 and Table S4). As for the QS-related
198 genes, *rhlI* had a mild induction and the *pqs* operon (including *pqsA/B/C/D/E*) had a strong up-regulation
199 (Table S4), suggesting RooA* induced the activation of both Rhl and PQS. Similar to the inactivating
200 MexT, RpoA* also substantially decreased the expression of the *mexEF-oprN* operon encoding the RND
201 efflux pump. Suppression of the MexEF-OprN pump caused by *mexT* mutations has been reported to
202 lead to QS reprogramming in the LasR-null background (Kostylev et al., 2019; Lamarche and Déziel,
203 2011; Oshri et al., 2018). We next compared the transcriptome profile between the LasR-MexT mutant
204 and the LasR-RpoA* mutant. Given the most up-regulated genes caused by *mexT* mutations are MexEF-
205 OprN pump-dependent (Tian et al., 2009a), we selected induced genes with at least 4-fold up-regulation
206 in the LasR-MexT mutant for further analysis. Genome-wide gene expression analysis revealed that those
207 genes strongly up-regulated in the LasR-MexT mutant were also enriched in the LasR-RpoA* mutant (P
208 $= 0.01$, one-sided KS test), but not for the genes down-regulated ($P = 0.07$, one-sided KS test). Taken
209 together, our results showed that RpoA* induced QS activation in the LasR-null background and a
210 decreased expression of the MexEF-OprN efflux pump, and suggested an efflux pump-induced QS-
211 active transcriptome profile analogous to the inactivating MexT.

212

213 **RpoA* directly represses the transcription of the MexEF-OprN efflux pump**

214 We used a transcriptional fusion GFP reporter (P*mexEF*-GFP) to monitor the RpoA*-mediated
215 transcriptional change of the *mexEF-oprN* operon. In line with the result of RNA-seq, RpoA* caused a
216 sharp reduction of the P*mexEF*-GFP (Fig. 5A), indicating a repressed MexEF-OprN effluxe pump.
217 Furthermore, as the inactivating MexEF-OprN pump stimulates the bacterial swarming motility
218 (Lamarche and Déziel, 2011), RpoA* consistently expanded the swarming movement (Fig. S5). Of note,
219 the LasR-RpoA* mutant showed an intermediate expression of the efflux pump between the LasR-null
220 mutant and the LasR-MexT mutant. Because the MexEF-OprN pump negatively regulates QS activity
221 (Lamarche and Déziel, 2011), a weak QS phenotype was observed in the LasR-RpoA* mutant relative
222 to the LasR-MexT mutant (Fig. 3). We next sought out to investigate how RpoA* attenuates the activity
223 of the MexEF-OprN pump. As RpoA is a transcriptional governor, we hypothesized that RpoA* may
224 directly interfere with the binding of RNAP to the promoter of the *mexEF-oprN* operon. To test this
225 hypothesis, we performed an electrophoretic mobility shift assay (EMSA) assay. We recombinantly
226 expressed and purified RNAPs from strain PAO1 either containing the wild-type RpoA or the point-
227 mutated RpoA*. Both types of RNAPs were tested for their binding to the probe DNA that harbors the
228 core promoter of *mexEF-oprN* (Fig. 5B). These RNAPs efficiently bound to the assayed probe (Fig. 5C).
229 In contrast to the wild-type RpoA, RpoA* reduced the RNAP-probe interaction. We therefore concluded
230 that RpoA* down-regulates the activity of the MexEF-OprN efflux pump by reducing the direct contact
231 of RNAP to the promoter DNA.

232

233 **PQS transport contributes to RpoA*-mediated QS activation**

234 Previous findings showed that inactivation of the MexEF-OprN efflux pump up-regulates the QS activity
235 by reducing the export of the PQS precursor (Köhler et al., 2001; Lamarche and Déziel, 2011). We
236 inferred that RpoA* may activate QS in a similar manner. This was supported by the strong induction of
237 the *pqs* operon shown in RNA-seq (Fig. 4B). We asked the question whether PQS accumulation is
238 responsible for the RpoA*-mediated QS-reprogramming. Given that *pqsA* codes for a coenzyme ligase
239 essential for PQS biosynthesis (Déziel et al., 2004), we deleted *pqsA* from the LasR-RpoA* mutant and
240 evaluated the resulting QS phenotypes. The *pqsA* deletion greatly but not completely diminished the QS-
241 controlled protease activity (Fig. S6). The effects of PQS observed in the LasR-RpoA* mutant are
242 reminiscent of those in the LasR-MexT mutant. Deletion of *pqsA* from the LasR-MexT mutant also did
243 not fully eliminate QS activity (Kostylev et al., 2019). Therefore, inactivating MexT and RopA* both
244 partially rely on PQS to rewire QS activity. Taken together, our data demonstrated that PQS transport
245 contributes to the RpoA*-mediated QS-reprogramming.

246

247 **The LasR-RpoA* mutant is more resistant to chloramphenicol**

248 We next investigated the clinical meanings of the LasR-RpoA* background, in which a higher expression
249 of the MexEF-OprN efflux pump and a lower QS activity relative to the LasR-MexT mutant. Since the
250 active MexEF-OprN efflux pump promotes antibiotics resistance (Köhler et al., 1997; Ko¨ hler et al.,
251 1997), we hypothesized that in the presence of antibiotics, the LasR-RpoA* mutant would be fitter than
252 the LasR-MexT mutant. To test this hypothesis, we used the LasR-null mutant to compete against either
253 the LasR-MexT mutant or the LasR-RpoA* mutant in the casein-based broth with or without antibiotic
254 treatment. In the absence of antibiotics, the LasR-MexT mutant outcompeted the LasR-null mutant (Fig.
255 6), in agreement with the previous report that the functioning QS in the LasR-MexT mutant provides the

256 competitive advantage (Oshri et al., 2018). Likewise, the LasR-RpoA* mutant exhibited a growth
257 advantage over the LasR-null mutant. We next conducted this competition assay exposed to varying
258 concentrations of chloramphenicol, a substrate modulated by the MexEF-OprN pump (Maseda et al.,
259 2000). In the presence of chloramphenicol, this efflux pump is important for the bacterium to acquire
260 antibiotic resistance. Our study found that with increased concentrations of chloramphenicol, the growth
261 advantage of either the LasR-MexT mutant or the LasR-RpoA* mutant over the LasR-null mutant was
262 quickly eliminated. In particular, the growth fitness declined slower in the LasR-RpoA* mutant than in
263 the LasR-MexT mutant. This competition results showed that in the QS-required condition, the LasR-
264 RpoA* mutant is more resistant to chloramphenicol than the LasR-MexT mutant when cocultured with
265 the LasR-null mutant.
266
267 **Further discovery of QS-reprogramming regulators**
268 To further identify unknown QS-reprogramming genetic determinants, we conducted another round of
269 evolution with the same LasR-null recombinant strain bearing dual-*mexT*. In this batch experiment, we
270 found that QS-active colonies had mutations in *gshA*, which encodes a glutamate-cysteine ligase. We
271 further illustrated that like RpoA*, the GshA mutant could also reprogram the QS hierarchy in the LasR-
272 null background in a MexEF-OprN-dependent manner (detailed description in the accompanying
273 manuscript). This novel functional role of GshA in QS-reprogramming has not yet been realized before.
274
275 **Iterative application of the DAGB approach**
276 We are curious and aim to dig out more QS-reprogramming genetic determinants. To this end, we
277 iteratively applied the DAGB approach. We introduced another copy of *rpoA* into the dual-*mexT*-
278 containing strain, generating a new recombinant LasR-null strain simultaneously bearing dual-*mexT* and
279 dual-*rpoA*. With this strategy, we hypothesized that spontaneous mutations for inactivating either *mexT*
280 or *rpoA* would be blocked during evolution, allowing for quick identification of QS-reprogramming
281 determinants that are none-*mexT* and none-*rpoA*. The new recombinant LasR-null strain was likewise
282 evolved and screened for QS-active phenotypes. Our study found that QS-active colonies had mutations
283 in *mexE*, coding for a membrane fusion protein of the MexEF-OprN pump (Ko¨ hler et al., 1997). Like
284 MexT, disruption of MexE could also induce QS-reprogramming in the LasR-null mutant (Kostylev et
285 al., 2019). Combining our findings, MexT, RpoA, GshA and MexE are either positive regulators or direct
286 components of the MexEF-OprN efflux pump (Fig. 7), suggesting the critical role of the MexEF-OprN
287 regulatory circuit in QS-reprogramming. Taken together, using DAGB-based iteration our research
288 further identified genetic determinants capable of reprogramming QS in the LasR-null background. More
289 importantly, our study set up an example for using DAGB-based iteration to identify underlying genetic
290 factors in other research fields in a broader spectrum of organisms (Fig. 8).
291
292 **Discussion**
293 Our study offers an innovative approach, named DAGB, for discovering unknown pathways or pathway
294 components in functional studies. Using DAGB, we first uncovered critical non-MexT regulators that
295 could reprogram the QS hierarchy in the *P. aeruginosa* LasR-null mutant. In a comparison of current
296 approaches, DAGB can rapidly identify untapped pathways or related components. For example, the QS-
297 reprogramming function of RpoA* could not be revealed if using the traditional transposon insertional
298 mutagenesis. Because *rpoA* is a housekeeping gene essential for cell viability (Lee et al., 2015), it could
299 not be arbitrarily inserted by the transposon element. As a starting point, the present study employed

300 DAGB to investigate unknown QS-associated factors in *P. aeruginosa*. We believe that the DAGB-based
301 approach has great potential to be broadly applicable to a wealth of related research fields in other
302 organisms. The application of DAGB would generate new opportunities for scientists to gain insight into
303 dark fields and yield fundamental discoveries.
304
305 Our study uncovers a novel QS-reprogramming role for RpoA*, deepening our functional understanding
306 of RpoA as a central transcriptional governor. Adaptive mutations in *rpoA* have been found to be
307 beneficial for bacterial growth in long-term evolution experiments in different organisms (Le Gac et al.,
308 2013; Rajaraman et al., 2016). Previous studies showed that *rpoA* mutations in *B. subtilis* and *E. coli*
309 promote the utilization of secondary carbon sources and ribosome synthesis (Murayama et al., 2015).
310 The QS-related function of RpoA* here implicates that specific residue substitution leads to a distinct
311 functionality configuration of RpoA. Our finding is in agreement with prior studies that certain residues
312 in the α-CTD domain of RpoA are important for promoter contact, while a subset of residues are
313 required for the interaction with transcriptional effectors (Finney et al., 2002; Gaal et al., 1996; Murakami
314 et al., 1996). This is demonstrated by our observation that RpoA* (T262->A) reduces the contacting of
315 the RNAP to the promoter of the *mexEF-oprN* operon (Fig. 5). All these combined findings suggest that
316 adjustment of the performance of RpoA through specific amino acid substitution allows for bacterial
317 quick adaptation to challenging environments.
318
319 Inactivation of the MexEF-OprN pump has been reported to lead to QS-reprogramming in the LasR-
320 MexT mutant (Kostylev et al., 2019; Oshri et al., 2018). Likewise, the RpoA* mutation identified in our
321 study could also activate QS activity in a MexEF-OprN-dependent manner. Transcriptome analysis,
322 EMSA and QS-controlled phenotypes collectively suggested that RpoA* affects the QS network through
323 the MexEF-OprN pump. MexEF-OprN-dependent QS activation relies on the transport of the PQS
324 precursor (Köhler et al., 2001; Lamarche and Déziel, 2011). However, deletion of key components of the
325 PQS system, such as PqsA and/or PqsE (Déziel et al., 2004; Diggle et al., 2006), only partially reduced
326 QS activity in the LasR-MexT mutant (Kostylev et al., 2019). How the MexEF-OprN pump shapes the
327 QS circuit awaits further classification. Similarly, the transport of the PQS molecule could not completely
328 account for RpoA*-mediated QS activation (Fig. S6).
329
330 RND family multidrug-resistance pumps promote *P. aeruginosa* resistance to a variety of antibiotics
331 (Schweizer, 2003). The *mexEF-oprN* operon codes for a typical RND efflux pump, which renders the
332 bacterium resistant to chloramphenicol, fluoroquinolones and trimethoprim (Lister et al., 2009).
333 Overexpression of the MexEF-OprN reduces QS activity (Köhler et al., 2001) due to the exportation of
334 the PQS precursor (Köhler et al., 2001; Lamarche and Déziel, 2011). Thus, the expression of the efflux
335 pump ultimately affects QS-controlled bacterial virulence. Previous studies found LasR-null, QS-active
336 isolates in the lungs of chronically infected CF patients (Bjarnsholt et al., 2010; Chen et al., 2019; Feltner
337 et al., 2016), where antibiotic treatments are rather common (Winstanley et al., 2016). This raises an
338 open question that how the bacterium solves the conflict between antibiotic resistance and QS activation.
339 In such a scenario, expression of the efflux pump is required for antibiotic resistance while impairing the
340 QS circuits that control the production of virulence factors. Our findings provide an insight into how the
341 bacterium solves this conflict. A single nucleotide substitution in the transcriptional governor RpoA
342 could postpone this conflict by fine-tuning the expression of the MexEF-OprN pump. This investment
343 tradeoff between antibiotic resistance and QS activation gave rise to a slower decline of growth fitness

344 in the RpoA* mutant when treated with chloramphenicol (Fig. 6). Therefore, a certain degree of
345 compromise between antibiotic resistance and QS regulation could be achieved by adjusting the
346 expression of the RND efflux pump.
347
348 *P. aeruginosa* has a complicated regulatory network (Huang et al., 2019) and undergoes evolutionary
349 changes in the process of chronic infections (Winstanley et al., 2016). This is reflected in our findings
350 that when inactivating MexT is not immediately available, the bacterium is able to quickly switch to
351 alternative pathways for achieving rapid QS activation. Given that the MexEF-OprN-independent
352 regulon of MexT is potentially important for bacterium-host interactions (Tian et al., 2009a; Tian et al.,
353 2009b), it is not hard to imagine that maintaining a wild-type MexT might be critical in certain clinical
354 environments. That perhaps explains previous observations that numerous LasR-null, QS-active isolates
355 from CF chronic infections remain functioning MexT (Cruz et al., 2020; Smith et al., 2006). Our findings
356 uncover non-MexT regulators that control the expression level of the MexEF-OprN efflux pump and
357 account for QS-reprogramming. Future studies need to classify the link between those non-MexT
358 regulators and specific clinical conditions.
359
360 **Materials and methods**
361
362 **Bacterial strains and growth**
363 *Pseudomonas aeruginosa* wild-type strain PAO1 and LasR-null mutant were obtained from E. Peter
364 Greenberg (University of Washington, USA). The PAO1 strain and the mutant derivatives were grown
365 in Luria Bertani (LB) broth containing 10 mg/ml tryptone, 5 mg/ml yeast extract, 10 mg/ml NaCl at 37°C.
366 LB broth was buffered with 50mM 3-(N-morpholino) propanesulfonic acid, pH 7.0 (LB-Mops broth).
367 The photosynthetic medium (PM) (Kim and Harwood, 1991) supplemented with 1% sodium caseinate
368 (PM-casein medium)(Cat. No. 9005-46-3, Sigmaaldrich, USA) as the sole carbon source was used for
369 evolution culture at 37°C. Unless otherwise specified, *P. aeruginosa* strains were cultured in 14-mm
370 FALCON tubes (Corning, USA) containing 3 ml medium, with shaking (220 RPM) at 37°C. *Escherichia*
371 *coli* was grown in LB broth at 37°C. Bacterial strains and plasmids used in this study are listed in
372 Supplementary Table S5.
373
374 **Construction of *P. aeruginosa* mutants**
375 Either point mutation or full gene knocking out was based on the homologous recombination exchange
376 approach as described previously (Rietsch et al., 2005). Briefly, about 500 ~ 1000 bp of DNA flanking
377 the targeted single nucleotide substitution or full length of gene of interest were PCR-amplified and
378 cloned into pEXG-2 vector (Gentamycin resistance, Gm) (Rietsch et al., 2005; Stover et al., 2000) with
379 the Vazyme ClonExpress II One Step Cloning kit (Vazyme Biotech, Nanjing, China), generating pEXG-
380 flanking constructs. The pEXG-flanking construct was mobilized into *P. aeruginosa* strain by triparental
381 mating with the help of *E. coli* PRK2013 strain (Kanamycin resistance, Km). Point mutation or deletion
382 mutants were first selected on *Pseudomonas* Isolation agar (PIA) containing 100 μg/ml gentamycin (Gm)
383 and further selected on LB agar containing 10% sucrose. All mutants were confirmed by PCR
384 amplification and subsequent DNA Sanger sequencing. The primers used in this study are listed in
385 supplementary TableS6.
386
387 **Complementation of the RpoA* mutant**

388 The *rpoA* gene was cloned into PJN105 expression vector with the Vazyme ClonExpress II One Step
389 cloning kit (Vazyme Biotech, Nanjing, China), generating plasmid PJN105-*rpoA*. The plasmid PJN105-
390 *rpoA* was mobilized into RpoA* mutant. The expression of RpoA in the complementation strain was
391 induced by adding 1mM L-arabinose and grown in LB-Mpos broth at 37ºC for 20 h.
392
393 **Evolution experiment**
394 Three independent colonies of recombinant LasR-null mutant bearing a miniTn7-MexT construct at the
395 neutral site of the genome were separately inoculated into 3 ml LB-Mops broth for overnight culture.
396 Cell evolution was initiated by transferring 100 μL bacteria grown in LB-Mops into 3 ml PM medium in
397 14-mm FALCON tubes (Corning, USA). Passage was performed every 5 days by exchanging 100 μL
398 bacteria into 3 ml fresh PM medium, and added sterile water replenish evaporated water in halfway. To
399 identify protease-positive variants, evolved colonies were isolated on LB agar and spotted onto the skim
400 milk plates at 37ºC for 24h to monitor the protease-catalyzed zones.
401
402 **Pyocyanin measurement**
403 Overnight cultures of *P. aeruginosa* grown in LB-mops broth were diluted into 4 ml *Pseudomonas* P
404 broth (20g/L pancreatic digest of gelatin,1.4g/L magnesium chloride,10g/L potassium sulfate) to reach a
405 starting $OD_{600} \approx 0.02$ and cultured at 37ºC for 20 h. The cells were spin down at 16,000 g × 2 min and
406 supernatants were measured at OD_{695} nm. Pyocyanin production was determined by plotting the OD_{695}
407 nm / OD_{600} nm over time.
408
409 **Cyanide measurement**
410 We used a cyanogenic test paper method to detect cyanide. The test paper is a circle of Whatman 3MM
411 chromatography paper soaked in the HCN detection reagent: copper(II) ethyl acetoacetate (5mg) and
412 4,4'-methylenebis-(N, N-dimethylaniline) (5 mg) in chloroform (1 to 2 ml). Briefly, cells grown
413 overnight in LB-Mops broth were used to spot-inoculate 2% peptone agar plates, and after 12 h at 37°C,
414 the plates were overlaid with test paper and incubated an additional 12 h at 37°C. The paper turns blue
415 when exposed to cyanide. The Image J software was used to quantify the production of hydrogen cyanide.
416
417 **Skim milk assay**
418 Total proteolytic activities of *P. aeruginosa* strains were evaluated through skim milk assay, in which
419 the tested strains form a zone of clearing on skim milk agar plate. Individual colonies were spotted on
420 the skim milk agar plates (25% LB, 4% skim milk, 1.5% agar). The protease-catalyzed zones were
421 photographed after incubation at 37°C for 24 h.
422
423 **Swarming motility assay.**
424 PAO1 strains were cultured in LB-Mops broth overnight to $OD_{600} \approx 1.8$. Then bacterial suspensions (1.5
425 μL; OD_{600} adjusted to 0.5) were added to agar plate (0.5% Bactor-agar, 8g/liter nutrient broth, and 5
426 g/liter glucose). Bacteria were incubated at 37°C for 16-18 h.
427
428 **Labelling of miniTn7-Gm**
429 The pUC18T-mini-Tn7T-Gm (NCBI accession number: AY599232) (Choi and Schweizer, 2006a) was
430 integrated into the neutral site of genome of PAO1 strains together with the transformation of helper
431 plasmid pTNS2 (NCBI accession number: AY884833). Integration event was confirmed by PCR

432 amplification and DNA sequencing. The excision of Gm resistance was performed with pFLP2 plasmid
433 (NCBI accession number: AF048702) (Choi and Schweizer, 2006b) and selected on LB agar containing
434 5% sucrose.
435
436 **Reporter assay**
437 P*rhlA*-GFP (Feltner et al., 2016) and P*pqsA*-GFP were used to quantified the RhlR- and PQS-responsive
438 activities, respectively. P*mexE*-GFP was used to assess the expression of the *mexEF-oprN* operon.
439 Reporter plasmids were mobilized into PAO1 strains and selected on LB agar plate (Gm). PAO1 strains
440 bearing QS reporter plasmids were grown in LB-Mops broth containing 50 mg/ml gentamycin for 12 h,
441 then diluted to LB-Mops broth (containing 50 mg/ml gentamycin) ($OD_{600} \approx 0.02$) and grown 18 h to
442 stationary phase and subsequently transferred to 96-well plates (200 ul/well) with three technique
443 replicates. The fluorescence (excitation 488 nm, emission 525 nm) and optical density (OD_{600}) of the
444 samples were recorded using a microplate reader machine (Synergy H1MF, BioTek Instruments,
445 Winooski, VT, USA).
446
447 **Quantification of C4-HSL and PQS**
448 *P. aeruginosa* strains were cultured overnight in LB-Mops broth. Bacteria with a starting $OD_{600} \approx 0.02$
449 were then grown in 4 ml LB broth at 37°C for 18 h. AHLs were extracted with equal amount of ethyl
450 acetate. Reporter *E. coli* strains containing pECP61.5 (Feltner et al., 2016) was used to quantify C4-HSL
451 in the ethyl acetate extract. Precise quantification of PQS was performed by LC/MS, as described
452 previously (Déziel et al., 2004). 10 µl of the ethyl acetate extraction sample was subjected into liquid
453 chromatography-mass spectrometry (LC-MS) detection system (Q-Exactive Focus/Ultimate 3000,
454 Thermo Scientific, USA) equipped with a 100*2.1mm,1.7 um ACQUITY UPLC HSS T3
455 chromatographic column (Waters, USA). 1% acidified water/methanol gradient was used as the mobile
456 phase at a flow rate of 0.4 ml min at 40°C. PQS was quantified by measuring the relative chromatographic
457 area of PQS molecular ions in different samples and multiplying by the concentration of the added
458 internal standard.
459
460 **Production and purification of RpoA variant protein**
461 Full-length of His-tagged RpoA or RpoA* variant was cloned into PJN105 expression vector and
462 overexpressed in the LasR-RpoA* mutant induced by 1mM L-arabinose at 37°C for 18 h. Cells were
463 pelleted at 13,000 g × 5 min and resuspended in lysis buffer (PBS supplemented with 1 ×Protease
464 Inhibitor Cocktail (Bimake, US), 1mg/ml lysozyme). Resuspended cells were lysed in high pressure
465 homogenizer machine (parameter 420 MPa, 4200 bar, Stansted Fluid power ltd, United Kingdom) and
466 pelleted at 13,000 g × 5 min at 4°C. The soluble fraction was incubated with Ni-NTA beads (Qiagene,
467 Shanghai, China) at 4°C for 2h. The mixture was loaded on a chromatographic column and washed with
468 low concentration of imidazole buffer (500 mM NaCl, 20 mM NaH_2PO4, 20mM imidazole, pH 8.0),
469 eluted with high concentration of imidazole buffer (500 mM NaCl, 20 mM NaH_2PO4, 250mM imidazole,
470 pH 8.0). Peak fractions were assessed by SDS PAGE analysis. Pooled fractions were concentrated with
471 ultrafiltration device (Millipore, USA) and eluted with PBS buffer, and stored at -80°C.
472
473 **Electrophoretic mobility shift assay (EMSA)**
474 The promoter sequence of the *mexEF-oprN* operon (P*mexE*) was used as probe for EMSA. The probe
475 DNA was labeled with biotin Biotin-11-UTP (Jena Bioscience, Germany) through PCR amplification

476 using T4 DNA polymerase (Novoprotein, China). The labeled probe (30 ng) was incubated with 0.2 μg
477 purified His-tagged RpoA or RpoA* in binding buffer (10 mM Tris-HCl, 50 mM KCl, 1 mM DTT, 1%
478 glycerin,10mM $MgCl_2$,1 μg/μL Poly (dI•dC), pH 7.5) at room temperature for 30min. DNA-protein
479 complex was subjected to electrophoresis on 5% polyacrylamide gel in 0.5×Tris-borate-EDTA (TBE)
480 buffer at 100 V for 180 min. DNA subsequently was transferred to a nylon membrane and incubated with
481 milk blocking buffer (50 g/L milk powder in TBST buffer, pH 7.5) for 30 min with shaking at room
482 temperature. The membrane was then incubated with streptavidin-horseradish peroxidase conjugate
483 (Thermo Scientific, USA) in blocking buffer for 30 min at room temperature. The membrane was
484 subsequently washed with TBST buffer (50 mM Tris, 150mM NaCl, 0.05% Tween-20, pH 7.5) for 4
485 time, 5 min each time. DNA was visualized using the Immobilon Western kit (Millipore, USA) and
486 photographed by Tanon 5200 Multi-Imaging System (Tanon, Shanghai, China).
487
488 **Mammalian cell cytotoxicity assay**
489 A549 cells were cultured in DMEM medium (GIBCO, USA) and F-12 medium (GIBCO, USA)
490 supplemented 10% FBS (GIBCO, USA), respectively, and maintained in 5% CO_2 at 37°C. Exponentially
491 growing bacteria (OD600≈1.0) in LB broth were washed with PBS and next were subjected to near-
492 confluent A549 cells at a starting multiplicity of infection (MOI) of 10: 1 and incubated at 37℃ for 8 h.
493 The extent of cell killing as determined by quantifying the release of lactate dehydrogenase in cell
494 supernatants with the LDH Cytotoxicity Detection Kit (Beyotime, Nantong, China).
495
496 **Competition experiment**
497 All assayed strains were grown in PM medium supplemented with 0.5% casein amino acid (Sangon,
498 Shanghai, China) for overnight and adjusted to OD_{600}≈0.02 in PM-Casein medium with or without
499 chloramphenicol. The strain tagged with pUC18T-mini-Tn7T-Gm cocultured with the unlabeled strain
500 at a starting ratio of 5:95. The mixed cells was then grown at 37°C for 48h. Cell counts were determined
501 by spreading bacteria onto LB agar plate with or without Gm-resistance. The relative fitness is calculated
502 as the ratio of Malthusian growth parameters (w) = $\ln(X_1/X_0)/\ln(Y_1/Y_0)$, according to previous definition
503 (Lenski et al., 1991).
504
505 **RNA extraction and sequencing**
506 PAO1 strains and derivatives were grown in LB-MOPS broth at 37°C for 18 h (OD_{600} ≈ 3.8-4.0). Total
507 RNA was isolated using TRIzol™ Reagent (ThermoFisher, HongKong, China). Total extracted quantity
508 was measured using NanoDropTM 1000 spectrophotometer (Thermo, US). Extracted RNA was DNase
509 treated (RQ1 RNase-free DNase I, Promega, Beijing, China) to remove genomic DNA contamination.
510 The obtained total RNA (2 independent RNA samples per strain) was sent for stranded paired-end
511 mRNA-seq sequencing in Novagen (Tianjin, China) using the Illumina Novaseq Platform.
512
513 **Quantitative real-time PCR (qRT-PCR)**
514 Total RNA of PAO1 strains and derivatives were reverse transcribed using the HiScript II 1st Strand
515 cDNA Synthesis Kit (Vazyme Biotech, Nanjing, China) following the manufacturer's instructions. The
516 obtained cDNA was used for qRT-PCR. Quantification reactions containing SYBR qPCR Master Mix
517 (Vazyme Biotech, Nanjing China) were prepared in 96-well plates and run in StepOnePlus Real-Time
518 PCR System (Applied Biosystems, USA) as recommended. Primers used for qRT-PCR are listed in Table
519 S6. The expression of targets of interest was normalized to the expression level of the *proC* gene.

520 Reactions were performed in triplicate.
521
522 **Transcriptome analysis**
523 RNA-seq short reads were filtered with a customized Perl script to remove Illumina adapters and low
524 quality of reads (Phred Score, Q < 30). The quality of filtered reads was assessed by FastQC. Trimmed
525 reads were then mapped to the *P. aeruginosa* PAO1 reference genome (NC_002516.2) using Hisat2. The
526 SAM files were further converted to BAM files by Samtools. Reads aligned to the reference genome
527 were counted by HTSeq. The generated count files were further processed un with the R package DESeq2.
528 Genes were regarded as "differentially expressed" if a fold change ⩾2.0 and a *P* value ⩽0.05.
529
530 **Gene expression profile analysis**
531 Genes showing expression 4-fold changes in strains were compared. *P* values were computed using a
532 one-sided KS test (Lim et al., 2005).
533
534 **Used Software**
535 The following software were used in this study.
536 BWA software, version 0.7.15-r1140 (http://bio-bwa.sourceforge.net) (Li and Durbin, 2009);
537 Cutadapt software, version 1.16 (https://github.com/mafdrcelm/cutadapt/) (Martin, 2011);
538 Samtools software, version 1.5 (http://samtools.sourceforge.net)(Li et al., 2009);
539 FastQC, version fastqc_v0.11.5 (https://www.bioinformatics.babraham.ac.uk/projects/fastqc/);
540 Hisat2, version 2.1.0 (https://daehwankimlab.github.io/hisat2/) (Kim et al., 2015);
541 HTSeq, version 0.11.1 (https://htseq.readthedocs.io/en/release_0.11.1/count.html) (Anders et al., 2015);
542 DESeq2 (Love et al., 2014);
543 Perl software, version v5.22.1 (https://www.perl.org/);
544 Python software, version v3.8.2 (https:// www. python. org/);
545 R software, version v3.6.1 (http://www.R-project.org/);
546 GraphPad Prism software, version 5 (https://www.graphpad.com/);
547 Image J software, version 1.8.0_172 (http://imagej.nih.gov/ij/).
548
549 **Statistical analysis**
550 Statistical analyses were performed using Excel and R software (http://www.R-project.org/).
551
552 **Data Availability**
553 RNA-seq data sets have been deposited in the NCBI SRA database (www.ncbi.nlm.nih.gov/sra) under
554 the accession number PRJNA863086.
555
556 **Authors' contributions**
557 W.C., H.L., M.L., X.Z., X.C. and W.D. designed experiments. W.C., H.L., M.L., X.Z., X.C. and W.D.
558 conducted the experiments. W.D. performed bioinformatics analyses. W.C. and W.D. wrote the
559 manuscript. All authors reviewed the manuscript.
560
561 **Competing interests**
562 The authors declare that they have no competing interests.
563

564 **Funding**
565 This work was supported by the National Natural Science Foundation of China (31771341).
566
567 **Acknowledgements**
568 We are grateful to Eugene Makeyev (King's College London, UK) for providing useful assistances in
569 bioinformatics analyses. We thank E. Peter Greenberg (University of Washington, USA) reading this
570 manuscript and giving useful comments. We want to express our gratitude to lab members for their
571 assistances and supports with respect to many aspects of this work.
572
573 **References**
574 Anders, S., Pyl, P.T., and Huber, W. (2015). HTSeq—a Python framework to work with high-throughput
575 sequencing data. *Bioinformatics 31*, 166-169.
576 Bjarnsholt, T., Jensen, P.Ø., Jakobsen, T.H., Phipps, R., Nielsen, A.K., Rybtke, M.T., Tolker-Nielsen,
577 T., Givskov, M., Høiby, N., and Ciofu, O. (2010). Quorum sensing and virulence of *Pseudomonas*
578 *aeruginosa* during lung infection of cystic fibrosis patients. *PloS one 5*, e10115.
579 Chen, R., Déziel, E., Groleau, M.-C., Schaefer, A.L., and Greenberg, E.P. (2019). Social cheating in a
580 *Pseudomonas aeruginosa* quorum-sensing variant. *PNAS 116*, 7021-7026.
581 Cheng, X., Lu, M., Qiu, H., Li, Y., Huang, L., and Dai, W. (2022). Spontaneous quorum-sensing
582 hierarchy reprogramming in *Pseudomonas aeruginosa* laboratory strain PAO1. *AMB Express 12*, 6.
583 Choi, K.-H., and Schweizer, H.P. (2006a). mini-Tn7 insertion in bacteria with single attTn7 sites:
584 example *Pseudomonas aeruginosa*. *Nature protocols 1*, 153.
585 Choi, K.-H., and Schweizer, H.P. (2006b). mini-Tn 7 insertion in bacteria with single att Tn 7 sites:
586 example *Pseudomonas aeruginosa*. *Nature protocols 1*, 153.
587 Cruz, R.L., Asfahl, K.L., Van den Bossche, S., Coenye, T., Crabbé, A., and Dandekar, A.A. (2020).
588 RhlR-regulated acyl-homoserine lactone quorum sensing in a cystic fibrosis isolate of *Pseudomonas*
589 *aeruginosa*. *MBio 11*.
590 Déziel, E., Lépine, F., Milot, S., He, J., Mindrinos, M.N., Tompkins, R.G., and Rahme, L.G. (2004).
591 Analysis of *Pseudomonas aeruginosa* 4-hydroxy-2-alkylquinolines (HAQs) reveals a role for 4-hydroxy-
592 2-heptylquinoline in cell-to-cell communication. *PNAS 101*, 1339-1344.
593 Diggle, S.P., Cornelis, P., Williams, P., and Cámara, M. (2006). 4-quinolone signalling in *Pseudomonas*
594 *aeruginosa*: old molecules, new perspectives. *Int J Med Microbiol 296*, 83-91.
595 Diggle, S.P., Griffin, A.S., Campbell, G.S., and West, S.A. (2007). Cooperation and conflict in quorum-
596 sensing bacterial populations. *Nature 450*, 411-414.
597 Feltner, J.B., Wolter, D.J., Pope, C.E., Groleau, M.-C., Smalley, N.E., Greenberg, E.P., Mayer-Hamblett,
598 N., Burns, J., Déziel, E., and Hoffman, L.R. (2016). LasR variant cystic fibrosis isolates reveal an
599 adaptable quorum-sensing hierarchy in *Pseudomonas aeruginosa*. *MBio 7*, e01513-01516.
600 Finney, A.H., Blick, R.J., Murakami, K., Ishihama, A., and Stevens, A.M. (2002). Role of the C-terminal
601 domain of the alpha subunit of RNA polymerase in LuxR-dependent transcriptional activation of the lux
602 operon during quorum sensing. *J Bacteriol 184*, 4520-4528.
603 Gaal, T., Ross, W., Blatter, E.E., Tang, H., Jia, X., Krishnan, V.V., Assa-Munt, N., Ebright, R.H., and
604 Gourse, R.L. (1996). DNA-binding determinants of the alpha subunit of RNA polymerase: novel DNA-
605 binding domain architecture. *Genes Dev 10*, 16-26.
606 Gellatly, S.L., and Hancock, R.E. (2013). *Pseudomonas aeruginosa*: new insights into pathogenesis and
607 host defenses. *Pathogens and disease 67*, 159-173.

608 Gilbert, J., OLIVAS, A., SHOGAN, B.D., VALUCKAITE, V., ZABORIN, A., BELOGORTSEVA, N.,
609 MUSCH, M., MEYER, F., TRIMBLE, W.L., and AN, G. (2012). Intestinal tissues induce an SNP
610 mutation in *pseudomonas aeruginosa* that enhances its virulence: possible role in anastomotic leak. *PloS*
611 *One 7*.
612 Hoffman, L.R., Kulasekara, H.D., Emerson, J., Houston, L.S., Burns, J.L., Ramsey, B.W., and Miller,
613 S.I. (2009). *Pseudomonas aeruginosa* lasR mutants are associated with cystic fibrosis lung disease
614 progression. *Journal of Cystic Fibrosis 8*, 66-70.
615 Huang, H., Shao, X., Xie, Y., Wang, T., Zhang, Y., Wang, X., and Deng, X. (2019). An integrated
616 genomic regulatory network of virulence-related transcriptional factors in *Pseudomonas aeruginosa*.
617 *Nature communications 10*, 1-13.
618 Köhler, T., Epp, S.F., Curty, L.K., and Pechère, J.-C. (1999). Characterization of MexT, the regulator of
619 the MexE-MexF-OprN multidrug efflux system of *Pseudomonas aeruginosa*. *J Bacteriol 181*, 6300-
620 6305.
621 Köhler, T., Michea-Hamzehpour, M., Plesiat, P., Kahr, A.-L., and Pechere, J.-C. (1997). Differential
622 selection of multidrug efflux systems by quinolones in *Pseudomonas aeruginosa*. *Antimicrobial agents*
623 *and chemotherapy 41*, 2540-2543.
624 Köhler, T., Van Delden, C., Curty, L.K., Hamzehpour, M.M., and Pechere, J.-C. (2001). Overexpression
625 of the MexEF-OprN multidrug efflux system affects cell-to-cell signaling in *Pseudomonas aeruginosa*.
626 *J Bacteriol 183*, 5213-5222.
627 Kim, D., Langmead, B., and Salzberg, S.L. (2015). HISAT: a fast spliced aligner with low memory
628 requirements. *Nat Methods 12*, 357-360.
629 Kim, M.-K., and Harwood, C.S. (1991). Regulation of benzoate-CoA ligase in *Rhodopseudomonas*
630 *palustris*. *FEMS Microbiol Lett 83*, 199-203.
631 Klockgether, J., and Tümmler, B. (2017). Recent advances in understanding *Pseudomonas aeruginosa*
632 as a pathogen. *F1000Research 6*.
633 Ko¨ hler, T., Michéa ‐ Hamzehpour, M., Henze, U., Gotoh, N., Kocjancic Curty, L., and Pechère, J.C.
634 (1997). Characterization of MexE–MexF–OprN, a positively regulated multidrug efflux system of
635 *Pseudomonas aeruginosa*. *Mol Microbiol 23*, 345-354.
636 Köhler, T., Van Delden, C., Curty, L.K., Hamzehpour, M.M., and Pechere, J.-C. (2001). Overexpression
637 of the MexEF-OprN multidrug efflux system affects cell-to-cell signaling in *Pseudomonas aeruginosa*.
638 J Bacteriol *183*, 5213-5222.
639 Kostylev, M., Kim, D.Y., Smalley, N.E., Salukhe, I., Greenberg, E.P., and Dandekar, A.A. (2019).
640 Evolution of the *Pseudomonas aeruginosa* quorum-sensing hierarchy. *PNAS 116*, 7027-7032.
641 Kulasekara, H.D., Ventre, I., Kulasekara, B.R., Lazdunski, A., Filloux, A., and Lory, S. (2005). A novel
642 two ‐ component system controls the expression of *Pseudomonas aeruginosa* fimbrial cup genes. *Mol*
643 *Microbiol 55*, 368-380.
644 Lamarche, M.G., and Déziel, E. (2011). MexEF-OprN efflux pump exports the *Pseudomonas* quinolone
645 signal (PQS) precursor HHQ (4-hydroxy-2-heptylquinoline). *PloS one 6*, e24310.
646 Le Gac, M., Cooper, T.F., Cruveiller, S., Médigue, C., and Schneider, D. (2013). Evolutionary history
647 and genetic parallelism affect correlated responses to evolution. *Mol Ecol 22*, 3292-3303.
648 Lee, J., and Zhang, L. (2015). The hierarchy quorum sensing network in *Pseudomonas aeruginosa*.
649 *Protein & cell 6*, 26-41.
650 Lee, S.A., Gallagher, L.A., Thongdee, M., Staudinger, B.J., Lippman, S., Singh, P.K., and Manoil, C.
651 (2015). General and condition-specific essential functions of *Pseudomonas aeruginosa*. *PNAS 112*,

652 5189-5194.
653 Lenski, R.E., Rose, M.R., Simpson, S.C., and Tadler, S.C. (1991). Long-term experimental evolution in
654 *Escherichia coli.* I. Adaptation and divergence during 2,000 generations. *The American Naturalist 138*,
655 1315-1341.
656 Li, H., and Durbin, R. (2009). Fast and accurate short read alignment with Burrows–Wheeler transform.
657 *Bioinformatics 25*, 1754-1760.
658 Li, H., Handsaker, B., Wysoker, A., Fennell, T., Ruan, J., Homer, N., Marth, G., Abecasis, G., and Durbin,
659 R. (2009). The sequence alignment/map format and SAMtools. *Bioinformatics 25*, 2078-2079.
660 Lim, L.P., Lau, N.C., Garrett-Engele, P., Grimson, A., Schelter, J.M., Castle, J., Bartel, D.P., Linsley,
661 P.S., and Johnson, J.M. (2005). Microarray analysis shows that some microRNAs downregulate large
662 numbers of target mRNAs. *Nature 433*, 769-773.
663 Lister, P.D., Wolter, D.J., and Hanson, N.D. (2009). Antibacterial-resistant *Pseudomonas aeruginosa*:
664 clinical impact and complex regulation of chromosomally encoded resistance mechanisms. *Clin*
665 *Microbiol Rev 22*, 582-610.
666 Love, M.I., Huber, W., and Anders, S. (2014). Moderated estimation of fold change and dispersion for
667 RNA-seq data with DESeq2. *Genome Biology 15*, 550.
668 Luong, P.M., Shogan, B.D., Zaborin, A., Belogortseva, N., Shrout, J.D., Zaborina, O., and Alverdy, J.C.
669 (2014). Emergence of the P2 phenotype in *Pseudomonas aeruginosa* PAO1 strains involves various
670 mutations in *mexT* or *mexF*. *J Bacteriol 196*, 504-513.
671 Martin, M. (2011). Cutadapt removes adapter sequences from high-throughput sequencing reads.
672 *EMBnet journal 17*, 10-12.
673 Maseda, H., Yoneyama, H., and Nakae, T. (2000). Assignment of the substrate-selective subunits of the
674 MexEF-OprN multidrug efflux pump of *Pseudomonas aeruginosa*. *Antimicrobial agents and*
675 *chemotherapy 44*, 658-664.
676 Murakami, K., Fujita, N., and Ishihama, A. (1996). Transcription factor recognition surface on the RNA
677 polymerase alpha subunit is involved in contact with the DNA enhancer element. *The EMBO Journal 15*,
678 4358-4367.
679 Murayama, S., Ishikawa, S., Chumsakul, O., Ogasawara, N., and Oshima, T. (2015). The role of α-CTD
680 in the genome-wide transcriptional regulation of the *Bacillus subtilis* cells. *PloS one 10*, e0131588.
681 Oshri, R.D., Zrihen, K.S., Shner, I., Omer Bendori, S., and Eldar, A. (2018). Selection for increased
682 quorum-sensing cooperation in *Pseudomonas aeruginosa* through the shut-down of a drug resistance
683 pump. *ISME J 12*, 2458-2469.
684 Papenfort, K., and Bassler, B.L. (2016). Quorum sensing signal–response systems in Gram-negative
685 bacteria. *Nat Rev Microbiol 14*, 576.
686 Rajaraman, E., Agarwal, A., Crigler, J., Seipelt-Thiemann, R., Altman, E., and Eiteman, M.A. (2016).
687 Transcriptional analysis and adaptive evolution of *Escherichia coli* strains growing on acetate. *Appl*
688 *Microbiol Biotechnol 100*, 7777-7785.
689 Richardot, C., Juarez, P., Jeannot, K., Patry, I., Plésiat, P., and Llanes, C. (2016). Amino acid
690 substitutions account for most MexS alterations in clinical nfxC mutants of *Pseudomonas aeruginosa*.
691 *Antimicrobial agents and chemotherapy 60*, 2302-2310.
692 Rietsch, A., Vallet-Gely, I., Dove, S.L., and Mekalanos, J.J. (2005). ExsE, a secreted regulator of type
693 III secretion genes in *Pseudomonas aeruginosa*. *PNAS 102*, 8006-8011.
694 Sandoz, K.M., Mitzimberg, S.M., and Schuster, M. (2007). Social cheating in *Pseudomonas aeruginosa*
695 quorum sensing. *PNAS 104*, 15876-15881.

696 Schweizer, H.P. (2003). Efflux as a mechanism of resistance to antimicrobials in *Pseudomonas*
697 *aeruginosa* and related bacteria: unanswered questions. *Genet Mol Res 2*, 48-62.
698 Smith, E.E., Buckley, D.G., Wu, Z., Saenphimmachak, C., Hoffman, L.R., D'Argenio, D.A., Miller, S.I.,
699 Ramsey, B.W., Speert, D.P., and Moskowitz, S.M. (2006). Genetic adaptation by *Pseudomonas*
700 *aeruginosa* to the airways of cystic fibrosis patients. *PNAS 103*, 8487-8492.
701 Sobel, M.L., Neshat, S., and Poole, K. (2005). Mutations in PA2491 (*mexS*) promote MexT-dependent
702 mexEF-oprN expression and multidrug resistance in a clinical strain of *Pseudomonas aeruginosa*. *J*
703 *Bacteriol 187*, 1246-1253.
704 Stover, C.K., Pham, X.Q., Erwin, A., Mizoguchi, S., Warrener, P., Hickey, M., Brinkman, F., Hufnagle,
705 W., Kowalik, D., and Lagrou, M. (2000). Complete genome sequence of *Pseudomonas aeruginosa*
706 PAO1, an opportunistic pathogen. *Nature 406*, 959-964.
707 Tian, Z.-X., Fargier, E., Mac Aogain, M., Adams, C., Wang, Y.-P., and O'Gara, F. (2009a).
708 Transcriptome profiling defines a novel regulon modulated by the LysR-type transcriptional regulator
709 MexT in *Pseudomonas aeruginosa*. *Nucleic Acids Res 37*, 7546-7559.
710 Tian, Z.-X., Mac Aogain, M., O'Connor, H.F., Fargier, E., Mooij, M.J., Adams, C., Wang, Y.-P., and
711 O'Gara, F. (2009b). MexT modulates virulence determinants in *Pseudomonas aeruginosa* independent
712 of the MexEF-OprN efflux pump. *Microb Pathog 47*, 237-241.
713 Winstanley, C., O'Brien, S., and Brockhurst, M.A. (2016). *Pseudomonas aeruginosa* evolutionary
714 adaptation and diversification in cystic fibrosis chronic lung infections. *Trends Microbiol 24*, 327-337.
715
716 **Figure legends**
717
718 **Figure 1. Scheme illustrating strategy used for the identification of QS-reprogramming genetic**
719 **determinants.**
720 Current strategy identified *mexT* as a QS-reprogramming regulator (top). Dual-acting-gene-blocking
721 (DAGB) strategy developed in our study (bottom), illustrating the steps to discover none-*mexT* QS-
722 regulators responsible for QS-reprogramming in the LasR-null background. QS-, inactive QS; QS+,
723 active QS.
724
725 **Figure 2. Evolution of the recombinant LasR mutant bearing dual-acting *mexT*.**
726 (A) Frequency of protease-positive colonies in the evolving population cells. Three independent
727 recombinant LasR-null mutants containing dual-acting *mexT* were initiated for evolution in the casein-
728 based broth. (B) Pyocyanin production in selected protease-positive colonies. Pyocyanin production was
729 quantified at OD_{695} divided by OD_{600} of each assayed strain, respectively. LasR-null, LasR-null mutant
730 as a negative control; LasR-1/2/3/4, evolved recombinant LasR mutant displaying protease-positive.
731 Data are presented as means ± SD ($n = 3$). *$P < 0.05$, **$P < 0.01$, ***$P < 0.001$ (t-test).
732
733 **Figure 3. Increased QS activity in the LasR-RpoA* mutant.**
734 (A-B) Rhl- (A) and PQS-responsive (B) QS activities in indicated strains. Rhl- and PQS-responsive QS
735 activities were reflected by the fluorescence levels of the reporter P*rhlA*-GFP and P*pqsA*-GFP,
736 respectively. Fluorescence expression were recorded as relative fluorescence unit (RFU) after 18h
737 incubation of indicated strains. (C-D) Relative concentration of C4-HSL(C) and PQS (D) in the assayed
738 strains. Productions of AHLs in wild-type (WT) PAO1 was set to 100%. (E) Pyocyanin productions in
739 assayed strains. Pyocyanin level was quantified at OD_{695} divided by OD_{600}. (F) Cyanide levels in

740 designated strains. Image J software was used to compare the amount of produced cyanide. Cyanide-
741 sensitive filter papers were photographed after post inoculation of bacteria 18h in the 6-well plate at 37
742 ^{o}C. The amount of cyanide produced in wild-type PAO1 was set to 100%. The experiment was repeated
743 three times and obtained results were similar. Data are presented as means ± SD (n = 3, t-test). *P <
744 0.05, **P < 0.01, ***P < 0.001 (t-test).
745
746 **Figure 4. Differentially expressed genes in the LasR-RpoA* mutant.**
747 (A) Volcano plots showing the magnitude of the differential gene expression induced by the RpoA*
748 mutation. Each dot represents one annotated sequence with detectable expression. Thresholds for
749 defining a gene significantly differentially expressed (log2(FoldChange) ≧|1.0|, P value ≦0.05) are
750 shown as dashed lines. Red dots, up-regulated genes; Blue dots, down-regulated genes; Green dots,
751 undifferentially expressed genes. (B-C) The expression levels of genes in QS genes (B) and the *mexEF-*
752 *oprN* operon (C). FoldChange in the expression of each indicated gene was calculated. Data are presented
753 as mean ± SD.
754
755 **Figure 5. RpoA* modulates the MexEF-OprN efflux pump.**
756 (A) RpoA* reduces the transcription of the *mexEF-oprN* operon. The transcriptional level of the *mexEF-*
757 *oprN* operon was reflected by the P*mexE*-GFP, a GFP reporter fused with the promoter sequence of *mexE*.
758 (B) Illustration of the probe DNA used for the Electrophoretic mobility shift assay (EMSA). (C) EMSA
759 assay showing RNAP containing wild-type (WT) RpoA or RpoA* bound to the probe DNA. The
760 unbound probe DNA and the DNA-protein complex are indicated by arrows. Data are presented as mean
761 ± SD. *P < 0.05, **P < 0.01, ***P < 0.001 (t-test).
762
763 **Figure 6. Effects of chloramphenicol on the growth fitness of the LasR-RpoA* mutant.**
764 The LasR-RopA* mutant or the LasR-MexT mutant labeled with Gm-resistance (pUC18T-mini-Tn7T-
765 Gm) was co-cultured with the LasR-null mutant at a start ratio of 5:95 and subjected to PM-casein
766 medium containing indicated concentrations of chloramphenicol for 48h. Colonies were counted and
767 relative fitness was computed as the ratio of Malthusian growth parameters (w).
768
769 **Figure 7. Graphic representation of the regulatory circuit of the MexEF-OprN efflux pump**
770 Illustration of the regulatory circuit of the MexEF-OprN efflux pump, containing the known MexT
771 transcriptional regulator and two new regulators identified in our study, RpoA (α-subunit of the RNAP)
772 and GshA.
773
774 **Figure 8. Iterative application of DAGB**
775 Schematic representation of the iterative application of the DAGB approach for identification of
776 unknown pathway components.
777
778 **Figure S1. Complementation of a wild-type RpoA into the LasR-RpoA* mutant reduces the QS-**
779 **controlled activity.**
780 Complementation of an episomal copy of wild-type *rpoA* gene in the LasR-RpoA* mutant diminished
781 the QS-controlled proteolytic activity (A) and the pyocyanin production (B). (A) Proteolytic activity
782 shown by the skim milk plate assay. Photographs were taken after inoculation of equal amount of bacteria
783 onto the skim milk plate and incubation for 24 hours at 37 ^{o}C. (B) Pyocyanin production of indicated

784 strains. The LasR-null mutant or the LasR-RpoA* mutant was either transformed with an empty vector
785 PJN105 (Ctr) or the RpoA-expressing vector PJN105-RpoA (RpoA). The RpoA expression was induced
786 by supplementation of L-arabinose (1 mg/ml). Data are from means ± SD (n = 3). *P < 0.05, **P <
787 0.01, ***P < 0.001 (t-test).
788
789 **Figure S2. Constructed LasR-RpoA* mutant exhibits elevated proteolytic activity.**
790 Proteolytic activity of designated strains. Equal amount of tested strains were spotted on to the skim milk
791 plate (A) and photographed after 24h of incubation. (B) Quantification of proteolytic zones in (A). Data
792 are from means ± SD (n = 3). *P < 0.05, **P < 0.01, ***P < 0.001 (t-test).
793
794 **Figure S3. RpoA* mutation significantly enhances host cell cytotoxicity.**
795 Human cell killing by mutant strains. Human lung carcinoma A549 were treated with indicated strains
796 in equal amounts. After 6h of inoculation, the relative cytosolic lactate dehydrogenase (LDH) was
797 quantified. The amount of LDH in wild-type PAO1 was set to 100%. Data are presented as means ±
798 SD (n = 3, t-test). *P < 0.05, **P < 0.01, ***P < 0.001 (t-test).
799
800 **Figure S4. qRT-PCR validation of differentially expressed genes obtained from the transcriptomic**
801 **analysis.**
802 Indicated genes were validated by qRT-PCR. Relative expression was normalized to the *proC* gene. Used
803 primers are shown in Table S6. Data are means ± SD (3 independent RNA extractions; n = 3). P-values
804 were obtained from t-tests. *P < 0.05, **P < 0.01, ***P < 0.001 (t-test).
805
806 **Figure S5. Swarming motility in the LasR-RpoA* mutant.**
807 (A)Bacterial swarming motility was assayed on 0.5% agar plate. Plates were photographed after 18h
808 incubation at 37 °C and representative photos are shown. (B) quantification of diameters in colonies. The
809 RpoA expression was induced by adding L-arabinose (1 mg/ml). LasR-null-Ctr, the LasR-null mutant
810 carrying an empty PJN105 vector; LasR-RpoA*-Ctr, the LasR-RpoA* mutant having an empty PJN105
811 vector; LasR-RpoA*-RpoA, the LasR-RpoA* mutant containing a PJN105-RpoA construct expressing
812 the wild-type RpoA. Data are means ± SD from a representative experiment (n = 3). P values were
813 obtained from t-test. *P < 0.05, **P < 0.01, ***P < 0.001. The experiment was repeated twice with
814 similar results.
815
816 **Figure S6. Deletion of PqsA reduces RpoA*-mediated QS activation.**
817 (A) Proteolytic activity was measured through spotting the same amount of indicated strains on the skim
818 milk plate. Plates were photographed after 24h incubation at 37 °C and representative photos are shown.
819 (B) quantification of proteolytic zone in (A). Data are from means ± SD (n = 3). *P < 0.05, **P < 0.01,
820 ***P < 0.001 (t-test).
821
822 **Supplementary Tables**
823
824 **Table S1. Mutations in lasR and mexT of isolates from chronically infected CF patients.**
825 **Table S2. Reads mapping statistics of whole-genome re-sequencing data.**
826 **Table S3. Identification of mutations in evolved protease-positive colonies.**
827 **Table S4. Genes differentially expressed in the LasR-RpoA* mutant.**

828 **Table S5. Strains and plasmids used in this study.**

829 **Table S6. Oligonucleotides used in this study.**

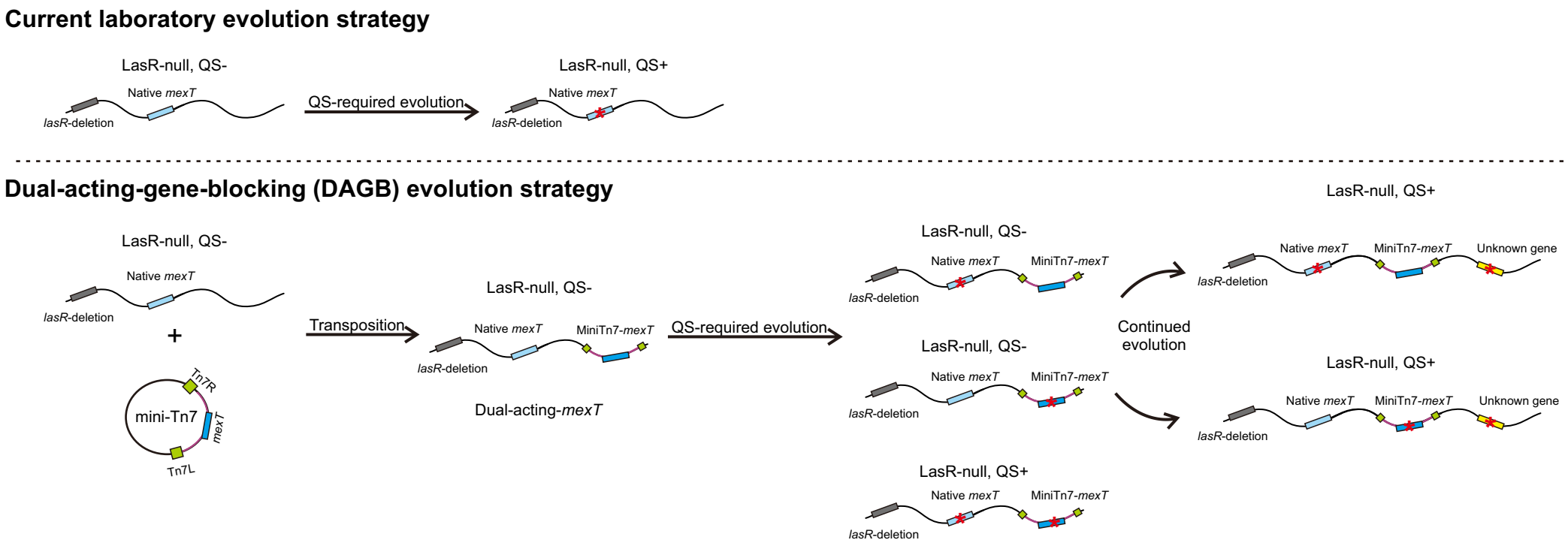
Current laboratory evolution strategy
LasR-null, QS-
Native mexT
lasR-deletion
QS-required evolution
LasR-null, QS+
Native mexT
lasR-deletion
Dual-acting-gene-blocking (DAGB) evolution strategy
LasR-null, QS-
Native mexT
lasR-deletion
+
Tn7R
mini-Tn7
mexT
Tn7L
Transposition
LasR-null, QS-
Native mexT
MiniTn7-mexT
lasR-deletion
Dual-acting-mexT
QS-required evolution
LasR-null, QS-
Native mexT
MiniTn7-mexT
lasR-deletion
LasR-null, QS-
Native mexT
MiniTn7-mexT
lasR-deletion
LasR-null, QS+
Native mexT
MiniTn7-mexT
lasR-deletion
Continued evolution
LasR-null, QS+
Native mexT
MiniTn7-mexT
Unknown gene
lasR-deletion
LasR-null, QS+
Native mexT
MiniTn7-mexT
Unknown gene
lasR-deletion

Fig. 1

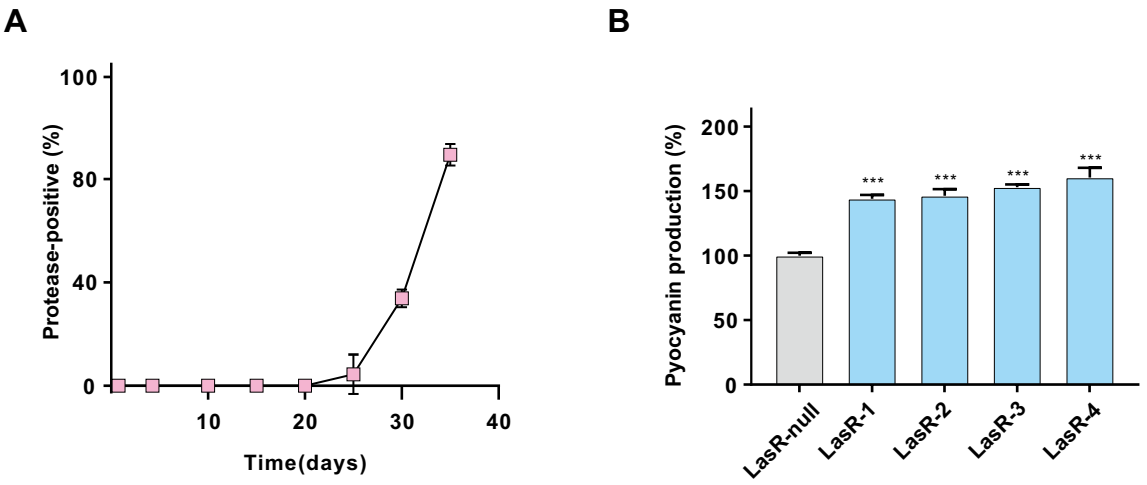
A
B
Protease-positive (%)
100
80
40
0
10
20
30
40
Time(days)
Pyocyanin production (%)
200
150
100
50
0
***
LasR-null
LasR-1
LasR-2
LasR-3
LasR-4

Fig.2

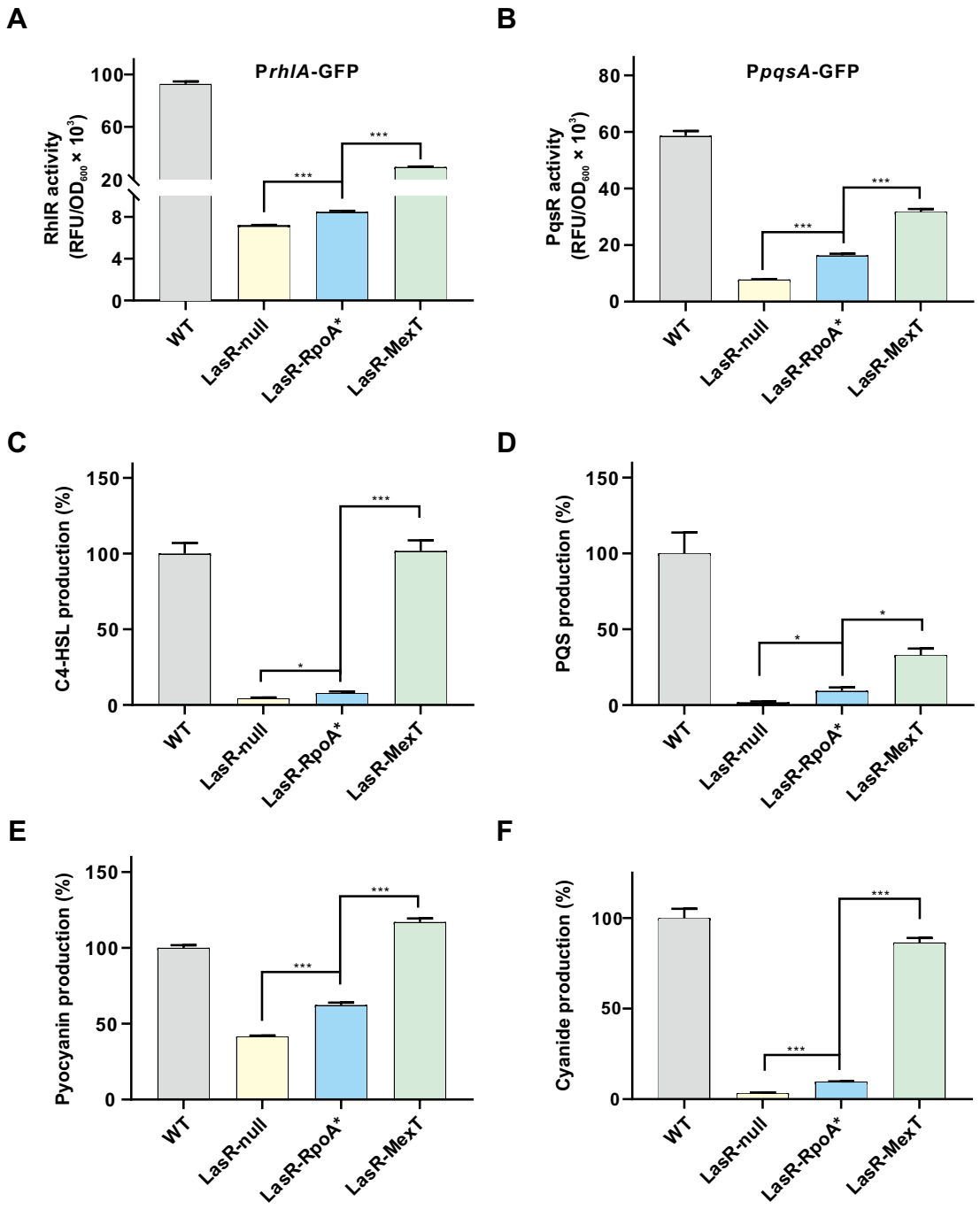
A
PrhlA-GFP
RhlR activity (RFU/OD600 × 10^3)
100
60
20
8
4
0
***
***
WT
LasR-null
LasR-RpoA*
LasR-MexT
B
PpqsA-GFP
PqsR activity (RFU/OD600 × 10^3)
80
60
40
20
0
***
***
WT
LasR-null
LasR-RpoA*
LasR-MexT
C
C4-HSL production (%)
150
100
50
0
*
***
WT
LasR-null
LasR-RpoA*
LasR-MexT
D
PQS production (%)
150
100
50
0
*
*
WT
LasR-null
LasR-RpoA*
LasR-MexT
E
Pyocyanin production (%)
150
100
50
0
***
***
WT
LasR-null
LasR-RpoA*
LasR-MexT
F
Cyanide production (%)
100
50
0
***
***
WT
LasR-null
LasR-RpoA*
LasR-MexT

Fig.3

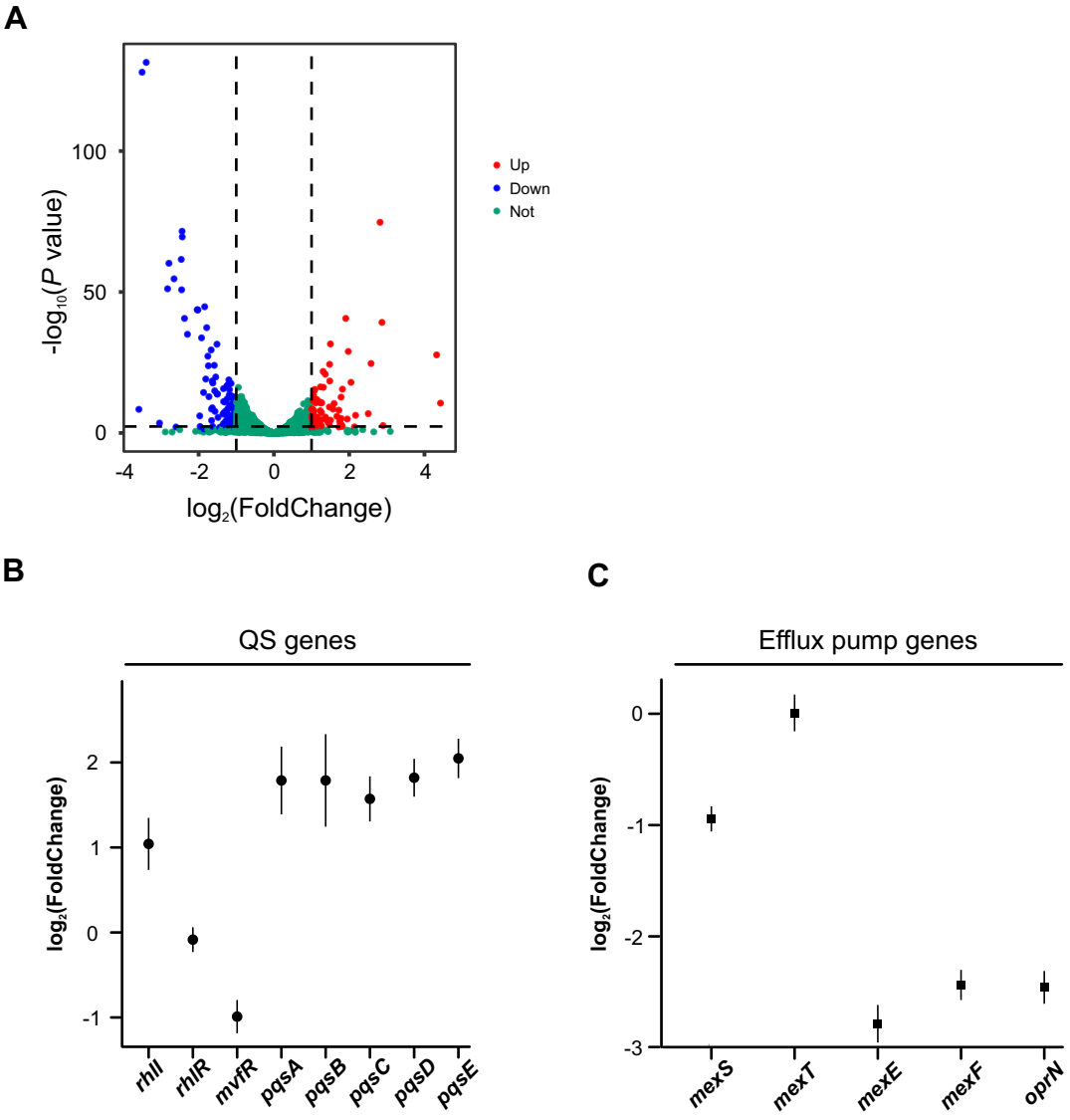
A
100
50
0
-4
-2
0
2
4
-log10(P value)
log2(FoldChange)
Up
Down
Not
B
QS genes
2
1
0
-1
log2(FoldChange)
rhlI
rhlR
mvfR
pqsA
pqsB
pqsC
pqsD
pqsE
C
Efflux pump genes
0
-1
-2
-3
log2(FoldChange)
mexS
mexT
mexE
mexF
oprN

Fig. 4

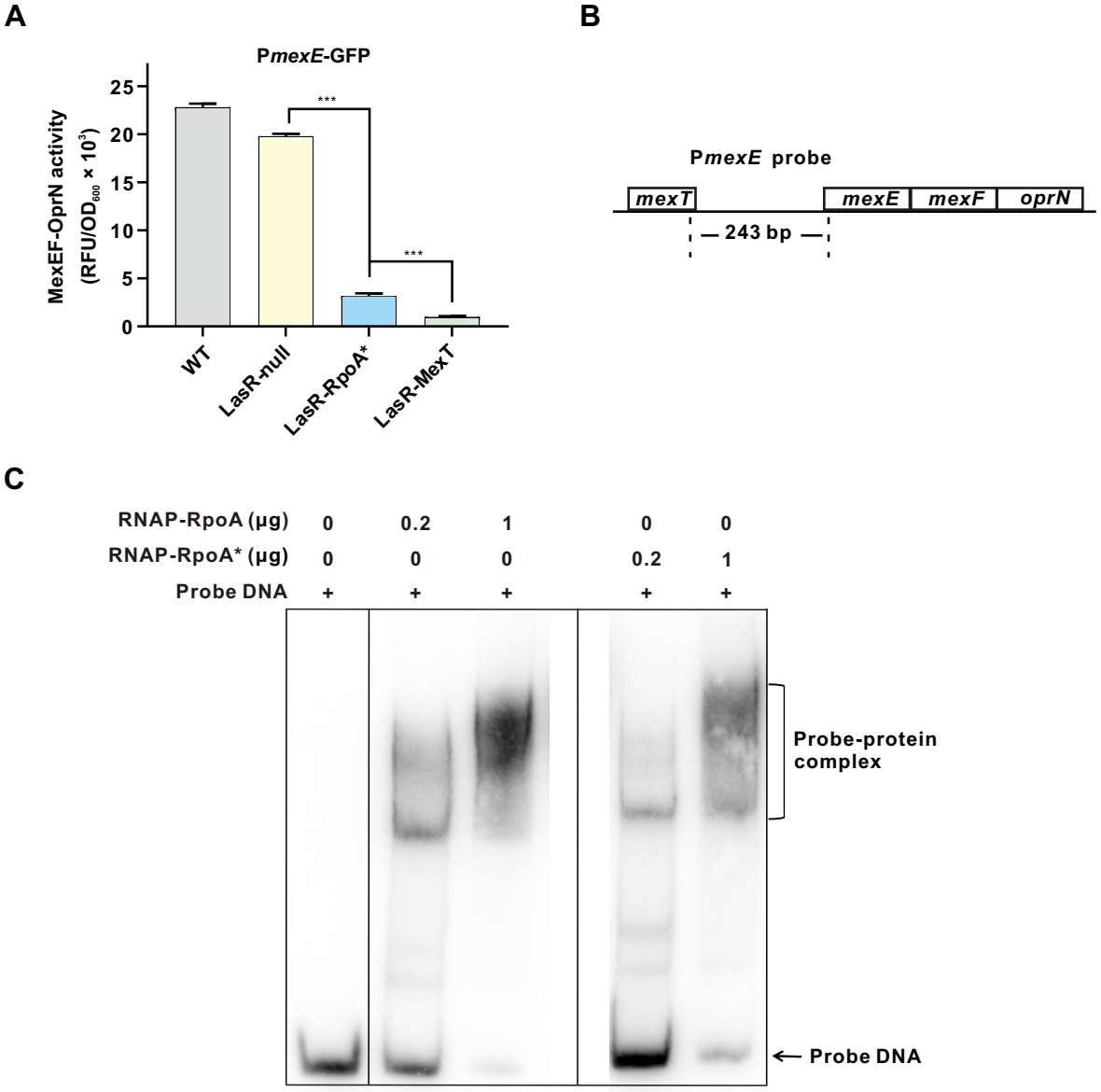
A
PmexE-GFP
MexEF-OprN activity
(RFU/OD600 × 10^3)
25
20
15
10
5
0
***
***
WT
LasR-null
LasR-RpoA*
LasR-MexT
B
PmexE probe
mexT
mexE
mexF
oprN
243 bp
C
RNAP-RpoA (μg) 0 0.2 1 0 0
RNAP-RpoA* (μg) 0 0 0 0.2 1
Probe DNA + + + + +
Probe-protein complex
Probe DNA

Fig. 5

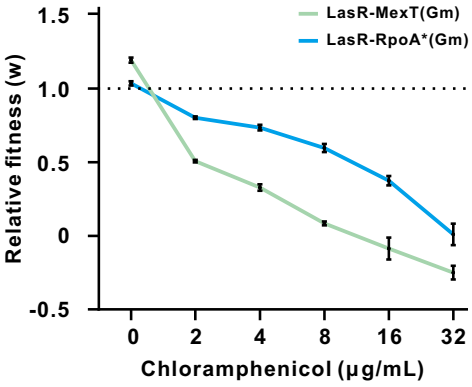
LasR-MexT(Gm)
LasR-RpoA*(Gm)
Relative fitness (w)
1.5
1.0
0.5
0
-0.5
0
2
4
8
16
32
Chloramphenicol (µg/mL)

Fig. 6

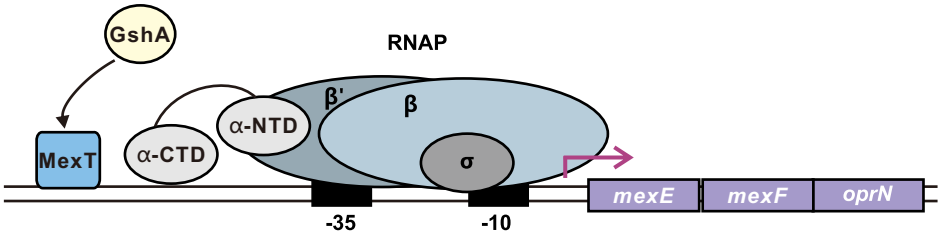

Fig.7

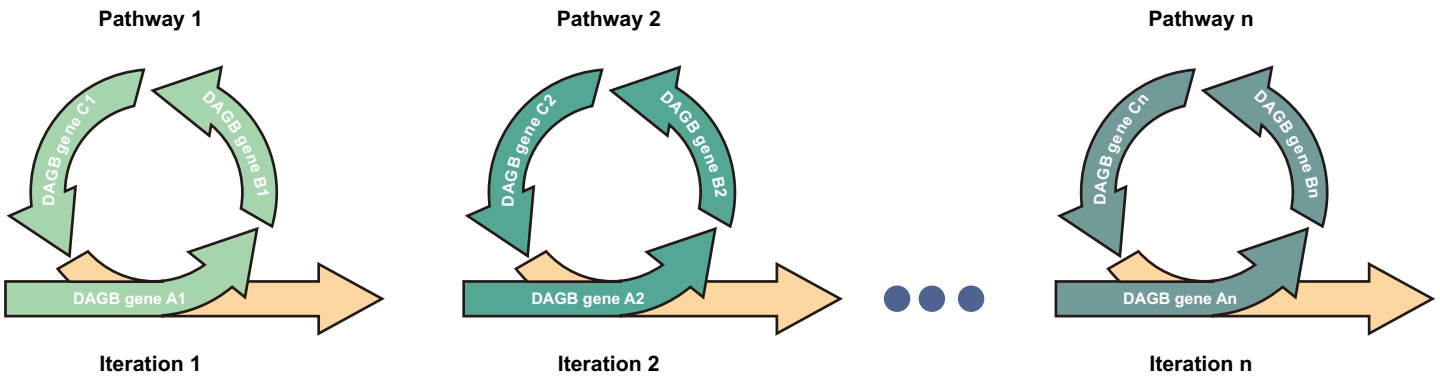
Pathway 1
DAGB gene C1
DAGB gene B1
DAGB gene A1
Iteration 1
Pathway 2
DAGB gene C2
DAGB gene B2
DAGB gene A2
Iteration 2
Pathway n
DAGB gene Cn
DAGB gene Bn
DAGB gene An
Iteration n

Fig. 8